Tuning the Solar Energy Storage Capacity of Dihydroazulene-Vinylheptafulvene (DHA-VHF) Molecular Switches: A DFT Study on Synergy of Substituent and Solvent effects on the Photochromic Properties

Azar Bagheri[a,*] and Malika Pejman[b]

[a]Department of Chemistry, CT.C., Islamic Azad University, Tehran, Iran,
[b]Faculty of Medicine, Iran University of Medical Sciences, Tehran, Iran.

***Corresponding author email:** azar.bagheri@iauctb.ac.ir

Received: Oct. 24, 2025, Revised: July 11, 2026, Accepted: July 25, 2026, Available Online: Oct. 11, 2026.
DOI: will be added soon.

ABSTRACT— The development of efficient molecular solar-thermal (MOST) energy storage systems and photochromic switches requires a profound understanding of the relationship between molecular structure and electronic properties. In this study, we systematically investigated the impact of various functional groups (-NH_2, –OMe, –Cl, –CN) and solvent environments (Gas phase vs. Aqueous phase) on the Dihydroazulene/ Vinylheptafulvene (DHA/ VHF) switching cycle using Density Functional Theory (DFT) and Time-Dependent DFT (TD-DFT) at the B3LYP/6-31G(d) level of theory. The importance of our system is due to the following reasons: 1. solar energy storage in chemical formore, 2. High reversibility, 3. Light - Controlled energy management, 4. Applications in sensors and photochromic materialsm, 5. Tunability through molecular engineering. The quantitative conversions of the photochemical forward reaction can be followed by NBO and spectral studies. In order to determine the optimized geometries, energies, dipole moments, atomic charges, thermochemical analysis and other properties. Through their strategic selection, it is possible to optimize the performance of smart materials and energy storage systems. Electron-donating and electron-withdrawing groups are key tools in molecular engineering. Our results demonstrate that electronic modulation via the phenyl ring's para-position significantly alters the HOMO-LUMO gap, with electron-donating groups (-NH_2 and -OMe) inducing a notable bathochromic (red) shift in the absorption spectra. Conversely, the electron-withdrawing cyanide (-CN) derivative enhances the electronic stability and global hardness of the VHF form, making it a superior candidate for long-term energy storage.Transition from the gas phase to an aqueous environment was found to dramatically increase the dipole moment and decrease the energy gap, suggesting that polar media facilitate the switching process and stabilize the polarized open-chain isomers. Natural Bond Orbital (NBO) analysis further confirms the role of n→π* and π→π* interactions in these structural transitions. Furthermore, the calculated NMR parameters (σiso and δ) serve as sensitive probes for identifying structural fingerprints, revealing a clear deshielding effect in the aqueous phase. In conclusion, while the -NH2 derivative is optimized for visible-light activation, the -CN derivative offers the best performance for thermal energy storage, providing a roadmap for the design of dual-purpose photoresponsive materials.

KEYWORDS: Dihydroazulene/Vinylheptafulvene (DHA/VHF), DFT/TD-DFT, Energy Storage (MOST), NMR Shielding, Solvent Effects, Substituent Effects.

I. INTRODUCTION

The dihydroazulene–vinylheptafulvene (DHA–VHF) system is one of the most extensively

[Downloaded from mail.ijop.ir on 2026-11-26]

studied photochromic molecular switches due to its reversible photo thermal isomerization and tunable physicochemical properties [1]-[7]. In this system, the closed ring dihydroazulene (DHA) isomer undergoes a photochemical ring opening reaction upon irradiation with ultraviolet or visible light to form the open chain vinylheptafulvene (VHF) isomer. The VHF form can subsequently revert thermally to the DHA structure, completing a reversible switching cycle. Because of the significant differences in electronic structure and absorption spectra between the two isomers, the DHA–VHF couple has attracted considerable attention in the fields of photochemistry and molecular materials.

Early investigations focused primarily on elucidating the photochemical mechanism of the DHA → VHF conversion and determining the spectroscopic characteristics of the two isomers. These studies demonstrated that the photoinduced transformation proceeds through an electrocyclic ring opening process in the excited state, followed by structural relaxation to the VHF form. Subsequent work explored the thermal back reaction (VHF → DHA) and revealed that the kinetics and stability of the VHF isomer are strongly influenced by molecular substitution and environmental conditions (Fig. 1).

A significant body of research has been devoted to the synthesis of substituted DHA derivatives in order to tune the photochemical and thermodynamic properties of the switching system. It has been shown that electron donating and electron withdrawing substituents can substantially modify the absorption spectra, quantum yields, and thermal half-lives of the VHF isomer. Such structural modifications have enabled improved control over switching efficiency and stability, making the DHA–VHF system a versatile platform for molecular design.

In recent years, the DHA–VHF system has attracted growing interest in the context of molecular solar thermal (MOST) energy storage. In these systems, solar energy is captured through photoisomerization of DHA to the higher energy VHF form, where the absorbed energy is stored in chemical bonds and can later be released through the thermally induced back conversion to DHA. This concept has motivated extensive experimental and theoretical studies aimed at increasing energy storage density, extending the lifetime of the VHF isomer, and shifting absorption toward the visible region of the solar spectrum.

Overall, the tunability, reversible photoresponse, and relatively high energy storage potential of the DHA–VHF system have made it a promising candidate for applications in photoresponsive materials, molecular switches, and solar thermal energy storage technologies. Continued efforts in molecular design, computational modeling, and photophysical characterization are expected to further enhance the performance and practical applicability of this class of photochromic compounds.

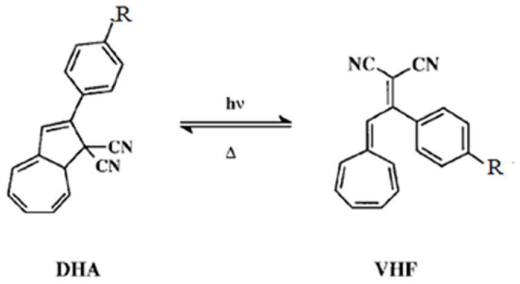


Fig. 1. photochromism in DHA-VHF (R=CN, OMe, Cl, NH_2).

DHA rearranges to the VHF upon irradiation, resulting in the appearance of electric current. However, the success of this approach depends on the choice of the set of active orbitals. For larger systems, single reference time dependent density functional theory (TD-DFT) is widely applied but its accuracy depends on the chosen functional and nature of the excited states

Surprisingly, there are very few studies devoted to the description of these electronic excited states and their implications on the UV-vis absorption spectra of the DHA and VHF isomers. This is most probably due to the notorious difficulty to have a balanced description of the electron correlation in excited states of different character. The challenge here

[Downloaded from mail.ijop.ir on 2026-11-26]

is to use advanced electronic structure methods capable of describing the electron correlation with the same relative accuracy in order to obtain reliable excitation energies and ordering of states of different nature

DFT calculations have served as a critical tool to understand and design organic small molecules for many applications in the field of photo electronics. Although many efforts have been made towards accurately describing UV-vis and fluorescence properties of organic small molecules, there are much needs to evaluate the accuracy of various functionals in description of electronic properties of organic small molecules.

DHAs undergo an interesting photoinduced rearrangement to the corresponding VHFs and this accompanied by a change of color form. In this study, we aim at describing and assigning the first absorption bands of the DHA/VHF couple. The photochromic properties of DHA systems are strongly dependent on the substituents on the five-membered ring, the solvent, and the temperature. In this study, calculations have been performed and compared for electron-donating and electron-withdrawing substituents. A detail understanding of this specific mechanism will help us design or improve new materials.

II. Materials and Methods

Geometerical optimizations and thermodynamic parameters calculations were done by Gaussian 09 software (Becke *et al.* 1993). [8],[9]. The calculations of systems contain C, O, and N atoms described by the standard 6-31G(d) basis set. Geometry optimization was performed utilizing with the Becke, three parameter, Lee-Yang-Parr method (B_3LYP) (O'Boyle *et al.* 2013). All NMR analysis have been performed using 6-31G(d) basis set and the B_3LYP level. The solvent effect was analyzed on the gas-phase optimized structures by means of the Polarizable Continuum Model with the integral equation formalism (PCM) [10],[11]. The GIAO methods was used to calculate the isotropic NMR shielding at the B_3LYP /6-31G(d) of theory. DOS plots calculated using the Gauss Sum 3.0 (Frisch *et al*., 2009; Lacy *et al*. 2005) Program package.

DFT-based chemical reactivity and stability descriptors which are chemical softness (S), electrophilicity (ω) and chemical hardness (η), electronic chemical potential (μ), were calculated as defined in equations 1-4 according to Koopmans theorem:

$$\mu = \left(\frac{\partial E}{\partial N}\right)_{V(r)\eta} \quad (1)$$

$$x\eta = \left(\frac{\partial^2 E}{\partial N^2}\right)_{v(r)I} \quad (2)$$

$$xS = \frac{I}{2\mu} \quad (3)$$

$$x\omega = \frac{\mu^2}{2\eta} \quad (4)$$

III. Results

In this study, the factors affecting the photochromism phenomenon of DHA-VHF have been investigated. In order to indicate the effects of electron-withdrawing-electron-donating factors, CN, Cl, OMe, NH_2 groups have been substituted for R in Fig. 1. Absolute energy values of these molecules, ionization potential (I), electron affinity (A), Energy gap and Chemical potential (μ), Global electrophilicity (ω) ΔNmax and Dipole Moment (debye) are gathered in Tables 1 and 2, in gas phases and the aqueous, respectively.

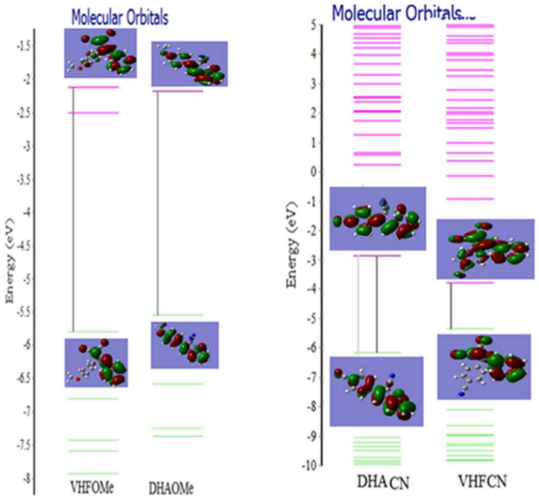


Fig. 2. Molecular Orbital diagrams DHA-OMe, VHF-OMe, DHA-CN and VHF-CN.

[Downloaded from mail.ijop.ir on 2026-11-26]

By carefully looking at the numbers in the solvent (water) section, we can see that the energy gap has changed relative to the gas phase. Polar solvents such as water usually stabilize the levels and, depending on the nature of the functional group, slightly change the gap, which is very important in predicting the behavior of the switch in biological environments or chemical solutions.

Table 1. The calculated amounts of Energy gap and Chemical potential (μ), Global electrophilicity (ω) ΔN_{max} Dipole Moment (debye) with the B3LYP/6-31G(d) basis set in gas and aquaeous phase for DHA derivatives.

Parameter		HOMO (au)	LUMO(a.u.)	η(eV)	μ	ω(eV)	ΔN(eV)	Gap Energy	Dipole (debye)
Gas phase	DHAOMe	_0.20395	_0.07988	0.062035	_0.141915	0.16233	2.287	0.12407	_0177269
	DHA-CN	_0.22627	_0.10395	0.06116	_0.16511	0.222868	2.699	0.12232	2.5238374
	DHA-NH_2	_0.19051	_0.07236	0.059075	_0.131435	0.14622	2.224	0.11815	_1.1611464
	DHA-Cl	_0.21512	_0.09167	0.061725	_0.153395	0.19061	2.485	0.12345	_1.0995436
Solvent= water	DHAOMe	_0.20081	_0.07996	0.060425	_0.140385	0.163077	2.323	0.12085	0.0395237
	DHA-CN	_0.22115	_0.10564	0.057755	_0.163395	0.096613	2.829	0.11551	3.519971
	DHA-NH_2	_0.19724	_0.08637	0.055435	_0.141805	0.18138	2.558	0.1108	_1.4080905
	DHA-Cl	_0.20840	_0.08604	0.06118	_0.14722	0.17713	2.406	0.12236	_1.578687

Table 2. The calculated amounts of Energy gap and Chemical potential (μ), Global electrophilicity (ω) ΔN_{max} Dipole Moment (debye) with the B_3LYP/6-31G(d) basis set in gas and aquaous phase for VHF derivatives.

Parameter		HOMO (au)	LUMO (a.u.)	η(eV)	μ	ω(eV)	ΔN(eV)	Gap Energy	Dipole(debye)
Gas phase	VHFOMe	_0.21335	_0.09195	0.0607	_0.15265	0.1919	2.514	0.1214	0.9165512
	VHF-CN	_0.21685	_0.11221	0.05232	_0.16453	0.2589	3.144	0.10464	3.2741681
	VHF-NH_2	_0.19986	_0.09126	0.0543	_0.14556	0.19509	2.680	0.1086	2.1415871
	VHF-Cl	_0.21153	_0.10518	0.053175	_0.158355	0.2358	2.977	0.10635	2.1185884
Solvent= water	VHFOMe	_0.20239	_0.09783	0.05228	_0.15011	0.21551	2.871	0.10465	2.169819
	VHF-CN	_0.2055	_0.10337	0.051065	_0.15443	0.2336	3.0242	0.10213	5.1250438
	VHF-NH_2	_0.20055	_0.09424	0.053155	_0.147395	0.20435	2.772	0.10631	3.8732869
	VHF-Cl	_0.20441	_0.10122	0.051595	_0.152815	0.2263	2.961	0.10319	3.6755669

Compounds with a smaller gap (such as amine derivatives) are considered softer. Soft molecules usually respond faster in photochemical reactions.

The -CN derivative has the highest Global Electrophilicity (ω) value. This means that it is an electron-hungry molecule, and this property can directly affect the stability of the VHF form and the thermal energy barrier of the reversal.

A. *Electronic Structure*

The energy gap between the frontier orbitals highest occupied molecular orbital (HOMO) and lowest unoccupied molecular orbital (LUMO) are significant properties in numerous chemical processes. The band gap is a good parameter for investigating the conductivity and reactivity of a compound. The energy values of the HOMO (E_{HOMO}) and LUMO (E_{LUMO}) reveals the electron donating and electron accepting characters of molecule, respectively. It has been explored in numerous investigations that the HOMO-LUMO gap may be a significant stability index of the molecules (Fig. 2).

The methoxy group (OMe) has raised the energy levels (especially the HOMO) by injecting electron density through resonance. Compared to other states, the energy gap here is usually smaller. This means that the absorption wavelength (λ_{max}) for the compound containing OMe should be larger (shifted to the red). If you look at the shape of the orbitals, the electron density in the HOMO is well spread over the phenyl ring and the oxygen of the methoxy group, which indicates the direct participation of this group in the π system.

[Downloaded from mail.ijop.ir on 2026-11-26]

The cyanide group (CN) has pushed the total energy levels towards more negative (lower) values due to its strong withdrawing properties (both inductive and resonant).The lowering of the levels indicates that the molecule is more resistant to oxidation and the VHF form in this case is usually more thermally stable (because the energy levels are in a more stable state).In the LUMO orbital, the electron density tends to be concentrated on the cyanide groups (both on the ring and on C1 number). The storage stability of the cyanide group form is greater and a shift to the blue side occurs.

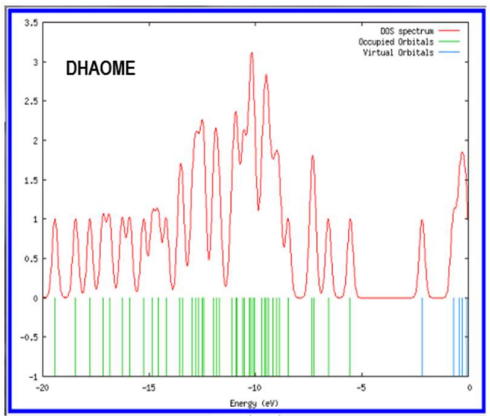
In order to better understand the electronic changes in the evaluated systems, density of states (DOS) curves was calculated (Fig. 3) It is also observed that the energy gap in the solvent phase is lower than in the gas phase. Studies show that in DHACN, the energy gap decreases with increasing the dielectric constant of the solvent, and in DHAOMe, changing the solvent does not have much effect on the energy gap. (Fig. 4).

Table 3. Comparison of dipole moments of DHA and VHF derivatives.

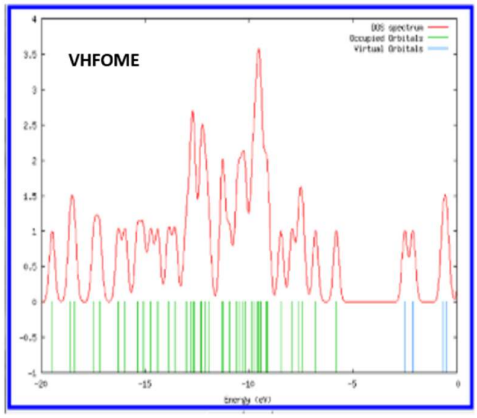
Components	Dipole moment
DHAOMe	2.9919
DHAOMe	7.7965
DHAOMe	5.2453
DHAOMe	5.4141
DHAOMe	8.0465
DHAOMe	10.2164
VHF-Cl	10.0139
VHF-NH_2	11.6491

B. *Dipole Moment*

Tomasi's polarized continuum model (PCM) defines the cavity as a union of represented numerically. PCM has proved usefulness in describing the effects of the solvent on some characteristic of the molecule in solution. A dipole in molecule will induce a dipole in medium, and the electric field applied by the solvent dipole will in turn interact with the molecular dipole, leading to net stabilization.



(a)



(b)

Fig. 3. (a) The density of states (DOS) plots of DHA-OMe (b) The density of states (DOS) plots of VHF-OMe.

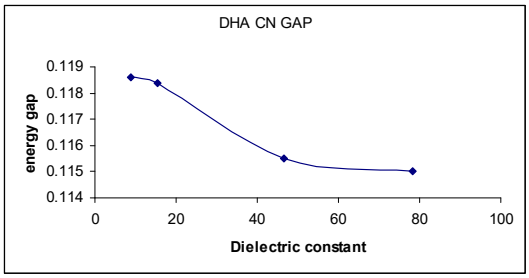


Fig. 4. Dielectric constant effect of the solvent on the energy gap DHA-CN.

The dipole moment is strongly dependent on the dielectric constant of the solvents and is greater than in the gas phase. The parameters have changed in water (Table 3).

The drastic changes in the Dipole column when converting DHA to VHF (shown in Table 2) indicate a "polarity switch". This large change in dipole moment means that this molecule can

[Downloaded from mail.ijop.ir on 2026-11-26]

be used in the design of sensors that are sensitive to environmental changes.

C. *Stabilization Energy*

The NBO analysis and second order Fock matrix are carried out by considering all possible interactions between (donor) Lewis NBOs and (acceptor) nonLewis NBOs. The intramolecular charge transfers (CT) or conjugations on the molecular backbone are the main features of photochromic properties of the molecules. For each donor NBO (i) and acceptor NBO (j), the resonance stabilization energy associated with $i \rightarrow j$ delocalization can be evaluated as:

$$E^2 = \Delta E_{ij} = q_i \frac{F(i,j)^2}{\varepsilon_j - \varepsilon_i} \quad (5)$$

where q_i is the donor orbital occupancy, ε_j and ε_i are diagonal elements and $F(i,j)$ is the off diagonal NBO Fock matrix element [12]. Donor-acceptor interaction and conjugation are key factors, which determine the photochromic properties of the compound. The results are tabulated in Tables 4-7.

Based on the functional groups used (-NH_2, -OMe, -Cl, -CN), the changes in E^2 in the DHA/VHF system are as follows:

1. Electron Donor Derivatives (-NH_2 and -OMe)

In these derivatives, the highest value of E^2 is observed. The non-bonding electron pairs (n) on nitrogen or oxygen pair with the antibonding orbitals π* of the phenyl ring and the dihydroazolene system. The effect is that the charge transfer from n-(N/O) →π*-ring increases the stability of the system and leads to the lowest energy gap that you see in the Tables. Usually E^2 for the amine derivative (NH_2) is larger than for the methoxy (OMe) because nitrogen is a better donor.

2. Electron-withdrawing derivative (-CN)

In this case, the direction of charge transfer and the type of orbitals involved are different. Here, the π orbitals of the ring act as donors and the π*orbitals of the cyanide group act as acceptors π-ring→π*-CN.

This interaction reduces the electron density on the ring. Although the stability energy E^2 is high in this direction, its nature makes the molecule "harder" (increased Hardness), which is evident in the gas phase Table.

One of the most interesting parts of our work is the comparison of E^2 between the two switch states. In the VHF form, due to the ring opening and expansion of the paired system (conjugation), the orbital overlap is better. Therefore, the total stability energy (E^2) in the VHF form is usually higher than in DHA.

The larger the value of E^2 in the VHF form for a particular derivative (such as -CN), the more electronically stable that molecule is in the open state and the better it stores energy (thermal stability).

In the aqueous phase Tables 6 and 7, it is observed that Polar solvents usually cause more polarization of the bonds, which can increase the E^2 values related to charge transfer (strengthening the interactions). This increase in stability due to charge transfer (E^2) is directly

related to the decrease in the HOMO-LUMO gap that you saw in the water Tables 4-7. Therefore, the order of E^2 for different derivatives is as follows:

-NH_2 (due to strong n→π*) resonance>-OMe>-CN (resulting in the stability of the VHF form)>-Cl. The bond lengths at the attachment to the side groups are reported in the Table 8. The stabilization energy for all the derivatives studied is given in the Table 8. It is observed that derivatives with electron withdrawing groups have higher charge transfer energy and derivatives with electron donating groups have lower charge transfer energy.

D. *Hybridation Coefficients*

Using the NBO output file and hybrid coefficients, we calculated the p orbital

[Downloaded from mail.ijop.ir on 2026-11-26]

The longer the bond length, the greater the degree of participation of the p orbital in the bond and, consequently, the lower the percentage of participation of the s orbital in it.

Table 4. The stabilization energy E^2 of DHA derivatives associated with delocalization for interaction that to give the strongest stabilization in B3LYP/6-31G(d) level in gas phase.

Parameters		E^2 (KCal /mol)	$E_j - E_i$(a.u.)	$F_{i,j}$(a.u.)	$q_{i,j}$
DHAOME	$BD(1)C_1 - C_2 \rightarrow BD^*(1)C_1 - C_4$	2.57	1.27	0.053	0.00347778
	$BD(1)C_{18} - C_{22} \rightarrow BD^*(1)C_{16} - C_{18}$	2.61	1.29	0.052	0.0032212
	$BD(1)C_{31} - N_{32} \rightarrow BD^*(1)C_{30} - C_{31}$	5.88	1.46	0.084	0.006498
DHA-CN	$BD(1)C_1 - C_2 \rightarrow BD^*(1)C_1 - C_4$	2.68	1.27	0.052	0.00334562
	$BD(1)C_{18} - C_{22} \rightarrow BD^*(1)C_{16} - H_{19}$	2.16	1.16	0.054	0.004232
	$BD(1)C_{32} - N_{33} \rightarrow BD^*(1)C_{22} - C_{32}$	6.54	1.56	0.090	0.006498
DHA-NH_2	$BD(1)C_1 - C_2 \rightarrow BD^*(1)C_1 - C_4$	2.74	1.27	0.053	0.00347778
	$BD(1)C_{18} - C_{22} \rightarrow BD^*(1)C_{16} - C_{18}$	2.83	1.29	0.054	0.00349448
	$BD(1)C_{30} - H_{31} \rightarrow BD^*(1)C_2 - C_3$	2.71	0.56	0.035	0.0078125
DHA-Cl	$BD(1)C_1 - C_2 \rightarrow BD^*(1)C_1 - C_4$	2.54	1.29	0.051	0.0031205
	$BD(1)C_{18} - C_{22} \rightarrow BD^*(1)C_{16} - C_{19}$	2.50	1.31	0.051	0.00302642
	$BD(1)C_{28} - N_{29} \rightarrow BD^*(1)C_{22} - C_{32}$	5.88	1.47	0.084	0.00652082

Table 5. The stabilization energy E^2 of VHF derivatives associated with delocalization for interaction that to give the strongest stabilization in B3LYP/6-31G(d) level in gas phase.

Parameters		E^2 (KCal /mol)	$E_j - E_i$(a.u.)	$F_{i,j}$(a.u.)	$q_{i,j}$
VHFOMe	$BD(1)C_1 - C_2 \rightarrow BD^*(1)C_1 - C_4$	3.16	1.26	0.056	0.00385442
	$BD(1)C_{19} - C_{21} \rightarrow BD^*(1)C_{16} - C_{19}$	3.22	1.32	0.058	0.003872
	$BD(1)C_{31} - N_{33} \rightarrow BD^*(1)C_{29} - C_{32}$	7.56	1.61	0.099	0.00753992
VHF-CN	$BD(1)C_1 - C_2 \rightarrow BD^*(1)C_1 - C_4$	2.80	1.25	0.053	0.00359552
	$BD(1)C_{19} - C_{21} \rightarrow BD^*(1)C_{16} - C_{19}$	2.42	1.27	0.050	0.00308898
	$BD(1)C_{32} - N_{33} \rightarrow BD^*(1)C_{21} - C_{32}$	6.40	1.56	0.090	0.00663552
VHF-NH_2	$BD(1)C_1 - C_2 \rightarrow BD^*(1)C_1 - C_4$	2.85	1.25	0.053	0.00359552
	$BD(1)C_{19} - C_{21} \rightarrow BD^*(1)C_{16} - C_{19}$	2.78	1.28	0.054	0.00354482
	$BD(1)N_{32} - H_{33} \rightarrow BD^*(1)C_{19} - C_{21}$	3.89	1.22	0.063	0.00516128
VHF-Cl	$BD(1)C_1 - C_2 \rightarrow BD^*(1)C_1 - C_4$	2.55	1.25	0.051	0.00332928
	$BD(1)C_{19} - C_{21} \rightarrow BD^*(1)C_{16} - C_{19}$	2.44	1.30	0.050	0.00294912
	$BD(1)C_{29} - C_{31} \rightarrow BD^*(1)C_{13} - C_{29}$	3.27	1.24	0.058	0.004436178

The p character of Cring in DHA-Cl /VHF-Cl (sp) is bigger than other derivatives (Table 9). So the C_{ring} -Cl bond length is longer (Table 8) participation rate using the DFT method and obtained the following results:

The longer the bond length, the greater the degree of participation of the p orbital in the bond and, consequently, the lower the percentage of participation of the s orbital in it. The p character of C_{ring} in DHA-Cl /VHF-Cl (sp) is bigger than other derivatives (Table 9) So the C_{ring} -Cl bond length is longer (Table 8).

E. *Population Analysis*

The Mulliken population analysis, like all atomic charge assignment schemes, is an arbitrary method for assigning atomic charges.

[Downloaded from mail.ijop.ir on 2026-11-26]

Generally, changes in the Mulliken population provide a reasonable estimation of changes in electron density within closely related molecules. Mulliken population analysis assigns atomic charges by dividing molecular orbital overlap even between each pair of atoms involved in a chemical bond.

Table 6. The stabilization energy E^2 of DHA derivatives associated with delocalization for interaction that to give the strongest stabilization in B3LYP/6-31G(d) level in water solvent.

Parameters		E^2(KCal/mol)	$E_j - E_i$(a.u)	$F_{i,j}$(a.u)	$q_{i,j}$
DHAOME Solvent= water	$BD(1)C_1 - C_2 \rightarrow BD^*(1)C_1 - C_4$	2.57	1.27	0.053	0.00347778
	$BD(1)C_{18} - C_{22} \rightarrow BD^*(1)C_{16} - C_{18}$	2.61	1.29	0.052	0.0032212
	$BD(1)C_{31} - N_{32} \rightarrow BD^*(1)C_{30} - C_{31}$	5.88	1.46	0.084	0.006498
DHA-CN	$BD(1)C_1 - C_2 \rightarrow BD^*(1)C_1 - C_4$	2.68	1.27	0.052	0.00334562
	$BD(1)C_{18} - C_{22} \rightarrow BD^*(1)C_{16} - H_{19}$	2.16	1.16	0.054	0.004232
	$BD(1)C_{32} - N_{33} \rightarrow BD^*(1)C_{22} - C_{32}$	6.54	1.56	0.090	0.006498
DHA-NH_2	$BD(1)C_1 - C_2 \rightarrow BD^*(1)C_1 - C_4$	2.74	1.27	0.053	0.00347778
	$BD(1)C_{18} - C_{22} \rightarrow BD^*(1)C_{16} - C_{18}$	2.83	1.29	0.054	0.00349448
	$BD(1)C_{30} - H_{31} \rightarrow BD^*(1)C_2 - C_3$	2.71	0.56	0.035	0.0078125
DHA-Cl	$BD(1)C_1 - C_2 \rightarrow BD^*(1)C_1 - C_4$	2.54	1.29	0.051	0.0031205
	$BD(1)C_{18} - C_{22} \rightarrow BD^*(1)C_{16} - C_{19}$	2.50	1.31	0.051	0.00302642
	$BD(1)C_{28} - N_{29} \rightarrow BD^*(1)C_{22} - C_{32}$	5.88	1.47	0.084	0.00652082

To identify any artifacts in the Mulliken population analysis, a natural bond orbital was also performed. Charge distributions of selected atoms were calculated by B_3LYP/6-31G* method (Tables 10 and 11). The natural charges of atoms in the functional groups provide information about the molecular polarizability, electronic structure and charge effects on the dipole moment. The results in Tables 10 and 11 show that in DFT study of DHA and VHF with decrease of charge of C22 atom in derivatives of CN, Cl, OMe and NH_2, charge of C, Cl, O and N decrease, respectively. Also, DHA-NH_2 the difference of atom charge of C22 and N is more than other DHA derivatives. This charge difference is less at VHF. Therefore, the bonds become weaker. The small interaction energy is also reflected in electron distribution at the atoms and the corresponding charges.

Analysis of the Mulliken Population Tables for DHA and VHF derivatives provides very important information about the distribution of electric charges on key atoms and how they change due to changes in the functional group and the environment (solvent).

In all Tables, the nitrogen and oxygen atoms of Electron Donating Groups (-NH_2, -OMe) have a significant negative charge. This indicates a high electron density that these atoms are ready to inject into the ring system. The carbon atoms -CN attached to this group show a different charge distribution, indicating that the electron cloud is pulled towards the nitrogen groups of the cyanide.

One of the most important observations in the Tables is the change in the charges of the molecule when moving from the gas phase to water. In the aqueous phase, positive charges become more positive and negative charges become more negative. This phenomenon indicates the solvent polarization effect. The polar solvent (water) causes more charge movement in the molecule to increase the dipole moment and increase the stability of the molecule in the solvent. This is completely consistent with the increase in the "dipole moment" (Tables 1 and 2).

A comparison of Tables 10 and 11 shows that ring opening (transformation of DHA to VHF) drastically changes the charge distribution of the central atoms. In the VHF case, due to the expansion of the paired system (π-conjugation), the charges are spread over the carbon atoms of the open chain (charge concentration in VHF). The carbon atoms that were involved in the

[Downloaded from mail.ijop.ir on 2026-11-26]

formation of the DHA ring (such as C22 or C21) experience a noticeable charge change after the ring opens, indicating a change in their hybridization and electronic environment.

Table 7. The stabilization energy E^2 of VHF derivatives associated with delocalization for interaction that to give the strongest stabilization in B3LYP/6-31G(d) level in water solvent.

Parameters		E^2(KCal/mol)	$E_j - E_i$(a.u)	$F_{i,j}$(a.u)	$q_{i,j}$
VHFOMe Solvent=water	$BD(1)C_1 - C_2 \rightarrow BD^*(1)C_1 - C_4$	3.16	1.26	0.056	0.00385442
	$BD(1)C_{19} - C_{21} \rightarrow BD^*(1)C_{16} - C_{19}$	3.22	1.32	0.058	0.003872
	$BD(1)C_{31} - N_{33} \rightarrow BD^*(1)C_{29} - C_{32}$	7.56	1.61	0.099	0.00753992
VHF-CN	$BD(1)C_1 - C_2 \rightarrow BD^*(1)C_1 - C_4$	2.80	1.25	0.053	0.00359552
	$BD(1)C_{19} - C_{21} \rightarrow BD^*(1)C_{16} - C_{19}$	2.42	1.27	0.050	0.00308898
	$BD(1)C_{32} - N_{33} \rightarrow BD^*(1)C_{21} - C_{32}$	6.40	1.56	0.090	0.00663552
VHF-NH_2	$BD(1)C_1 - C_2 \rightarrow BD^*(1)C_1 - C_4$	2.85	1.25	0.053	0.00359552
	$BD(1)C_{19} - C_{21} \rightarrow BD^*(1)C_{16} - C_{19}$	2.78	1.28	0.054	0.00354482
	$BD(1)N_{32} - H_{33} \rightarrow BD^*(1)C_{19} - C_{21}$	3.89	1.22	0.063	0.00516128
VHF-Cl	$BD(1)C_1 - C_2 \rightarrow BD^*(1)C_1 - C_4$	2.55	1.25	0.051	0.00332928
	$BD(1)C_{19} - C_{21} \rightarrow BD^*(1)C_{16} - C_{19}$	2.44	1.30	0.050	0.00294912
	$BD(1)C_{29} - C_{31} \rightarrow BD^*(1)C_{13} - C_{29}$	3.27	1.24	0.058	0.004436178

Table 8. Comparison of bond length and stabilization energy of components in attachment site Functional groups of R= OMe, CN, Cl and NH_2 to DHA or VHF.

Components	Length of bonds	E^2 (KCal /mol)
DHAOME	1.38	1.32
DHA-CN	1.42	6.10
DHA-Cl	1.75	2/77
DHA-NH_2	1.37	0.60
VHFOME	1.383	1.36
VHF-CN	1.431	6.06
VHF-Cl	1.755	2/76
VHF-NH_2	1.378	0.65

F. *Study of Chemical Shifts*

According to GIAO calculations performed, the σ_{iso} values of the NMR shielding tensor have been reported. Ab initio calculations yield the data in Tables 12 and 13 show the values for the isotropic shielding, chemical shifts anisotropy and chemical shifts anisotropy asymmetry and effective anisotropy. It is worth mentioning that the electrostatic properties of nuclei are mainly dependent on the electronic density around them. Therefore, side groups affect the electrical density of all nucleus.

The analysis of Tables 12 and 13, which are related to NMR parameters (nuclear shielding) including isotropic(σ_{iso}), anisotropy (δ) and asymmetry parameter (η) values for key atoms in both gas and aqueous phases, provides a very detailed view of the changes in the chemical environment of the atoms during the switching process.

1. Isotropic shielding (σ_{iso}) changes and solvent effect

The σ_{iso} values are directly related to the electron density around the nucleus. Comparing the two Tables 12 and 13, it is observed that for most atoms, the shielding value has changed in the aqueous phase relative to the gas phase. For example, in the DHA-NH_2 derivative for atom N32, the shielding change indicates the polarization of the C-N bond by water molecules.

For some carbon atoms, the σ_{iso} value has decreased in the aqueous phase. This means a reduction in electron density around the nucleus due to the electron attraction of the solvent or rearrangement of the electron cloud π which makes the nucleus "bare" and resonate at different frequencies.

2. Anisotropy (δ) and the spatial distribution of the electron cloud

The anisotropy parameter indicates the degree of non-sphericity of the electron distribution around the nucleus. In the VHF form (open structure), the anisotropy values at most of the main chain carbon atoms show large changes compared to DHA. This is due to the change in hybridization from sp3 (at the ring junction carbons) to sp2 and the expansion of π pairing.

In the aqueous phase, the anisotropy values change, indicating the influence of the

[Downloaded from mail.ijop.ir on 2026-11-26]

intermolecular forces of the solvent on the orientation of the electron cloud of the bonds.

3. Asymmetry parameter

This parameter indicates the deviation of the electron distribution from cylindrical symmetry.Values close to zero indicate high symmetry and values close to one indicate strong asymmetry of the chemical environment of the atom. In the Tables 12 and 13, atoms directly attached to functional groups (R) show the highest degree of asymmetry, which is fully consistent with the nature of donor-acceptor systems (Push-Pull).

Table 9. Hybridation coefficient of bonds calculated by NBO method in $b_3$lyp/6-31G*level.

Compounds	Bond	Phase and Solvent	Hybridation coefficients	Contribution of *p* orbital in σ bond
VHF-OMe	C21-O24	Gas phase	BD(1)=0.5791(sp3.07) C21+0.8153(sp2.19) O24	0.01873
		In water	BD(1)=0.8188(sp2.87) C21-0.5741(sp2.11) O24	0.03144
VHF-CN	C21-C32	Gas phase	BD(1)=0.7168(sp2.38) C21+0.6973(sp0.86) C32	0.03157
		In water	BD(1)=0.7000(sp2.38) C21-0.7142(sp0.86) C32	0.03084
VHF-Cl	C21-Cl32	Gas phase	BD(1)=0.6753(sp3.4) C21+0.7375(sp4.57) Cl32	0.03089
		In water	BD(1)=0.7706(sp3.5d 0.01) C21+0.7408(sp4.56d 0.03 sp3.5d 0.01) Cl32	1.9895
VHF-NH_2	C21-N32	Gas phase	BD(1)=0.6348 (sp2.49) C21+0.7727(sp1.53) N32	1.98943
		In water	BD(1)=0.7706(sp2.44) C21+0.6373(sp1.54) N32	0.01808
DHA-OMe	C22-O25	Gas phase	BD(1)=0.5737(sp3.08) C22+0.8190(sp2.13) O25	0.01918
		In water	BD(1)=0.5737(sp3.08) C22+0.8189(sp2.11) O25	0.03144
DHA-CN	C22-C32	Gas phase	BD(1)=0.7168(sp2.87) C22-0.6973(sp0.86) C32	0.03347
		In water	BD(1)=0.7013(sp2.87) C22-0.7129(sp0.86) O24	0.03055
DHA-Cl	C22-Cl32	Gas phase	BD(1)=0.6753(sp3.40) C22+0.7375(sp4.55) Cl32	0.03256
		In water	BD(1)=0.6715(sp3.48d 0.01) C22+0.7408(sp4.54d 0.03 sp3.5d 0.02) Cl32	1.9896
DHA-NH_2	C22-N32	Gas phase	BD(1)=0.7728(sp2.42) C22-0.6347(sp1.53) N32	1.98952
		In water	BD(1)=0.7697(sp2.42)C22-0.6384(sp1.61) N32	0.01745

4. Case analysis based on functional groups NMR data prove that the water solvent changes the chemical environment of the nuclei, resulting in a change in the charge distribution (observed in the mole charges) and a change in the stability of the orbitals. The conversion of DHA to VHF is accompanied by a huge structural change in the electron cloud π which is accurately tracked by the anisotropy parameter. The greatest effect of the solvent is on the "heteroatom" atoms (N and O) and the carbons attached to them, which represent active sites for interaction with the external environment.

The significant changes in the sigma of the iso at O25 in DHA-OMe indicate the interaction between water and the methoxy oxygen. The significant change in the shielding of N32 in DHA -NH_2 confirms the increased polar character of the NH_2 group in aqueous medium. The shift in the shielding of C21-C22 indicates the rearrangement of double bonds throughout the switch skeleton upon solubilization.

Table 10. Mulliken population of selected atoms in DHA derivatives in the gas phase and water solvent at the B_3LYP.

Compounds	Atom	Gas phase	Water solvent
DHAOME	C22	0.296109	0.294777
	O25	_0.557085	_0.578821
DHA-CN	C22	0.112613	0.037170
	C32	_0.049366	0.316432-
DHA-Cl	C22	_0.061512	_0.068019
	Cl32	_0.006488	_0.030433
DHA-NH_2	C22	0.345568	0.489329
	N32	_0.810140	_0.121463

The higher the coverage constant in the carbons of the benzene ring, the higher the coverage constant of the aromatic ring, so the aromaticity of the ring is higher, and also when the aromaticity of the ring is higher, the compound

[Downloaded from mail.ijop.ir on 2026-11-26]

is more stable. Studies have shown that ring carbon in the DHA-CN and VHF-CN derivatives have highest σ_{iso}, so their aromaticity is higher, so they are more stable.

Table 11. Mulliken population of selected atoms in VHF derivatives in the gas phase and water solvent at the B3LYP level.

Compounds	Atom	Gas phase	Water solvent
VHFOME	C21	0.260694	0.294274
	O24	_0.560268	_0.579180
VHF-CN	C21	0.107394	0.094327
	C32	_0.045052	_0.019365
VHF-Cl	C21	_0.06081	_0.064192
	CL32	_0.008439	_0.030560
VHF-NH_2	C21	0.339334	0.322936
	N32	_0.809081	_0.117561

Table 12. Comparison of isotropy and anisotropy and asymmetry of molecules in gas phase

Compounds	Functional group attachment site	Isotropic σ_{iso}	Anisotropy (δ)	Asymmetry
DHAOME	C22	36.55	131.523	_0.72035
	O25	206.774	92.0721	_1.364
DHA-CN	C22	81.839	137.768	_0.6047
	C32	77.412	321.474	0.3208
DHA-Cl	C22	51.061	110.740	_0.6164
	Cl32	714.024	438.668	_0.10010
DHA-NH_2	C22	55.0404	164.2186	_0.772081
	N32	195.254	73.6123	_0.24814
VHFOME	C21	38.655	136.206	_0.07798
	O24	248.7121	105.0814	0.8226
VHF-CN	C21	80.6480	140.4270	_0.29819
	C32	77.6315	321.8576	0.57884
VHF-Cl	C21	50.4813	112.8276	_0.28538
	Cl32	714.4581	449.5228	0.52777
VHF-NH_2	C21	53.9720	165.9051	_0.4287
	N32	195.9107	74.5818	0.87578

Table 13. Comparison of isotropy and anisotropy and asymmetry of molecules in aquaous phase.

Compounds	Functional group attachment site	Isotropic (σiso)	Anisotropy (δ)	Asymmetry
DHAOME	C22	36.5455	131.3900	_0.79809
	O25	208.1239	92.0788	_1.5028
DHA-CN	C22	85.6639	129.4526	_0.63602
	C32	74.9871	322.3510	0.04552
DHA-Cl	C22	52.6426	103.6372	_0.40792
	Cl32	725.8009	444.0743	_0.06313
DHA-NH_2	C22	50.3953	169.0817	_0.8475
	N32	192.3770	76.0446	_0.50603
VHFOME	C21	35.4384	133.9063	_0.00358
	O24	208.8161	88.1876	0.9398
VHF-CN	C21	82.6652	135.8622	_0.280029
	C32	74.9537	322.9362	0.56809
VHF-Cl	C21	50.9132	109.2234	_0.3276
	Cl32	725.3396	444.4722	0.52058
VHF-NH_2	C21	51.6382	169.9716	_0.42868
	N32	190.5860	68.9916	0.92249

[Downloaded from mail.ijop.ir on 2026-11-26]

Studies have shown that ring carbon in the DHA-CN and VHF-CN derivatives have highest σ_{iso}, so their aromaticity is higher, so they are more stable.

According to the data of the Table 14 in each of the two most phased energy terms (ΔH, and ΔG) is related to the CN source and this group has more stability and higher storage capacity It has high values that indicate drastic electronic changes in the system due to strong sound properties.The chlorine group (Cl) shows the lowest energy difference, confirming that halogen does not cause radical changes in the thermodynamics of this switch. Comparing the gas and aqueous phases in Table 14, a large jump in the numbers is observed. For example, Δ G values in the aqueous phase (e.g. for NH_2 from 5.08 to 13.55) increase by a factor of about 2 to 3 (increasing stability in aqueous media). The polar solvent strongly stabilizes the VHF form, which usually has a higher dipole moment. This means that in aqueous media, the energy barrier for returning to DHA becomes higher and the molecule can store energy for a longer period of time. H) Absorption properties

Electronic absorption is a very fast process and it is necessary to create switching devices that respond as quickly, the excited states of molecules can fluoresce, carry out electron and energy transfer, and cause bond formation and breaking. Each of these processes can be used for switching and data storage [13]. In this work, the photochromic behavior of the compounds was studied by TD-DFT calculations using CPCM (Figs. 5, 6). The results obtained from the UV-vis spectra are summarized in Table 15. The effect of the solvent on the optimized gas phase structures was also analyzed. Electronic absorption is a very fast process and it is necessary to create switching devices that respond as quickly, the excited states of molecules can fluoresce, carry out electron and energy transfer, and cause bond formation and breaking. Each of these processes can be used for switching and data storage [13]. In this work, the photochromic behavior of the compounds was studied by TD-DFT calculations using CPCM (Figs. 5, 6). The results obtained from the UV-vis spectra are summarized in Table 15. The effect of the solvent on the optimized gas phase structures was also analyzed.

Table 14. Comparison of ΔG،ΔH،ΔE in different derivatives in gas and aqueous phases

Parameters	Phase and Solvent	NH_2	Cl	CN	O-Me
-ΔG	**DHA-VHF (gas)**	5.08	1..82	5.08	5.02
	DHA-VHF (water)	13.554	0.0102	13.62	9.22
-ΔH	**DHA-VHF (gas)**	3.76	0.878	3.76	3.514
	DHA-VHF (water)	13.62	5.02	15.25	8.15
-ΔE	**DHA-VHF (gas)**	4.487	0.94	3.76	3.514
	DHA-VHF (water)	14.43	4.96	15.18	8.09

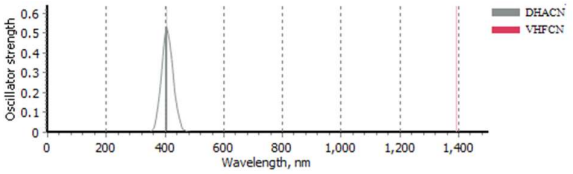
In both pairs of derivatives (OMe and CN), it is observed that by converting DHA to VHF, the main absorption peak is shifted towards longer wavelengths (Red-shift). The reason is that in the VHF structure, the conjugated system (Conjugation) is extended along the molecule. This extension reduces the energy gap between HOMO and LUMO and as a result, the electron transition takes place with lower energy (longer wavelength). For example, in the case of the OMe derivative, the absorption peak has shifted from about 396 nm in DHA to 414 nm in VHF. Our spectra show a drastic difference between the donor and the acceptor groups. The absorption peaks of the OMe derivative (donor) are located in the visible region near the ultraviolet (about 400 nm). This indicates that the presence of the methoxy group has greatly reduced the energy required for excitation by raising the HOMO level.

But in the spectrum of DHA-CN, a very sharp and narrow peak is seen. Cyanide groups tend to direct electronic transitions to specific energy regions due to their strong repulsion. According to Figs. 4 and 5, the peak shift in CN derivatives is different from that of OMe, indicating the strong influence of CN groups on the stability

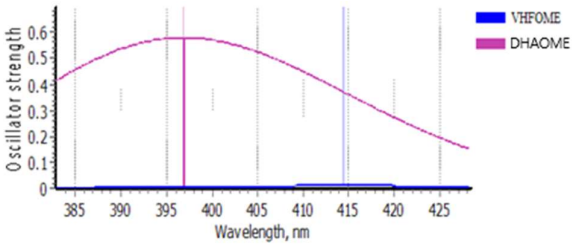
[Downloaded from mail.ijop.ir on 2026-11-26]

of the excited state. Absorption strength and extinction coefficient (ε) in the spectra. Vertical axis indicates the intensity of absorption. It can be seen from the figures that VHF forms generally have high extinction coefficients (longer peaks), which means high efficiency of light absorption in the open state. Oscillator Strength (f) indicates the probability of that electronic transition occurring. The larger this number, the stronger the absorption and the deeper the color of the solution. (e.g. f=0.5797 for DHA-OMe) According to the wavelengths of maximum (λ_{max}) the observed color is predicted | DHA-OMe | ~396 | UV-Visible boundary | Colorless or very light yellow || VHF-OMe | ~414 | Violet/Blue | Light yellow || VHF-CN | ~476 | Blue/Green | Orange/Red |.

It is important to note that in the VHF-CN derivative, the absorption peak is located near 476 nm. This means that this derivative absorbs well in the visible region and is a very efficient optical switch for working with visible light (instead of UV).



(a)



(b)

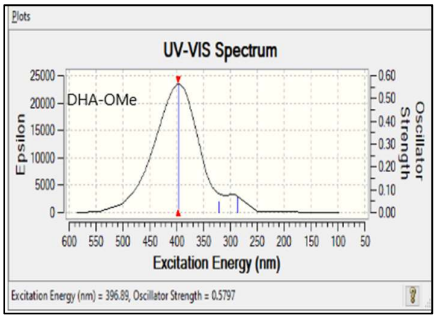
Fig. 5. UV-Visible optical absorption spectra of the studied a) Cyanide b) methoxy compounds calculated by TD/ DFT/ B_3LYP/6-31* G level in the gas phase.

The absorption spectra prove that this system is a true photochromic switch (clear change in λ_{max} upon photoexcitation).

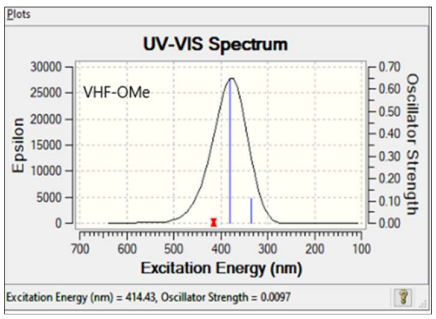
Derivatives with strong donor (OMe) and attractor groups (CN in the VHF form) give the best response in the visible region. The accuracy of TD-DFT calculations in reproducing the experimental trend (red-shift upon ring opening) is evaluated very well.

In all our samples, wherever the gap energy in the Tables is lower (such as -NH_2 and -OMe derivatives), the absorption peak in the UV-Vis spectra has moved towards longer wavelengths (Red-shift). This agreement between the data in Tables 1 and 2 with the spectral plots indicates the high validity of our calculations. Analysis of the energy difference (Gap vs. Excitation): Usually, the energy of the first electronic excitation (E_{ex}) is not exactly equal to the HOMO-LUMO gap, but is slightly less than it. The reason is that in TD-DFT calculations, the effects of "orbital relaxation" and "electron-hole interaction" in the excited state are taken into account, which are not present in simple DFT calculations. If you compare the value of E_{ex} (which is obtained from λ_{max}) with Gap, their difference indicates the energy of the Coulomb interaction in the excited state.

For example, the wavelength of 396 nm in DHA-OMe corresponds to an excitation energy of about 3.13 eV. If you compare this number with the gap energy column in the gas phase Table, you can gauge the accuracy of the B_3LYP method.

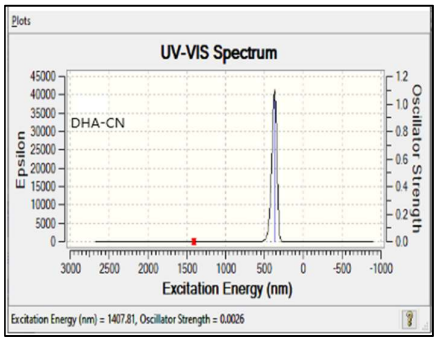


(a)

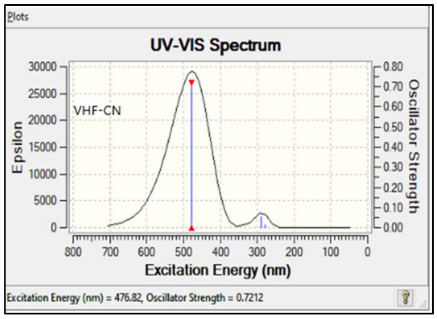


(b)

[Downloaded from mail.ijop.ir on 2026-11-26]



(c)



(d)

Fig. 6. UV-Visible optical absorption spectra of the studied a) DHAOMe b) VHFOMe c) DHACN d) VHFCN compounds calculated by TD/ DFT/ B3LYP/6-31* G level in water.

Table 5. Excitation energies of studied compounds.

Compounds	Solvent	Exaction en
DHA-OMe	Gas phase	1604
	In water	396.9
VHF-OMe	Gas phase	472
	In water	414
DHA-CN	Gas phase	400
	In water	1427
VHF-CN	Gas phase	1400
	In water	476

The wavelength of 476 nm in VHF-CN corresponds to 2.60 eV. The peak shift from the UV to the visible region (476 nm) shows that in this derivative, the energy gap has been reduced so much that the molecule is practically colored (orange/red).

IV. Discussion

Photochromic switches are examples of molecular switches in which configurational changes occur upon light excitation [14]-[16]. Light plays a fundamental role in the chemical conversion of energy and the control of molecular motion of the switchable compound. Light intensity and irradiation time affect the kinetics of the photochemical reaction [17]-[20]. For example, the ring-opening reaction of a DHA leads to the formation of a colored VHF, which involves significant changes in the electronic structure of the π system.This study aimed to investigate the effect of functional groups (–NH_2, –OMe, –Cl, –CN) and solvent (water) on the physicochemical properties of dihydroazolone/vinyl hephthalatefulone optical switch. The key results from DFT and TD-DFT calculations are as follows:

1. Electronic behavior and frontier orbitals

Effect of functional groups: Electron-donating groups (–NH_2, –OMe) reduce the energy gap by increasing the HOMO level and lead to a red shift in the absorption spectrum. In contrast, the electron-withdrawing group –CN increases the electronic stability of the VHF form by stabilizing the energy levels.

Hardness and softness: The derivatives containing –NH_2 showed the lowest hardness(η), indicating their high photoreactivity, while the –CN derivative had the highest hardness in the gas phase.

2. Effect of the environment (gas phase vs. aqueous phase)

The transition to the aqueous phase resulted in a sharp increase in the dipole moment in all derivatives. This indicates a better stability of the switch in polar environments. Molecular charge analysis also confirmed that the aqueous solvent increases the charge separation in the molecule and enhances the compressive-tensile nature of the system.

3. Optical and spectroscopic properties

Photochromic shift: TD-DFT calculations showed that the conversion of DHA to VHF with increasing the length of the coupling system leads to a decrease in the excitation energy and a shift of the absorption peaks to the visible region (photochromic shift). The VHF-CN derivative with an absorption peak around 476 nm was found to be the most efficient

[Downloaded from mail.ijop.ir on 2026-11-26]

derivative for use in visible light-based technologies.

4. Magnetic analysis (NMR)

Nuclear shielding: NMR results showed that the aqueous environment leads to a decrease in the shielding (σ_{iso}) of key atoms. This phenomenon (Deshielding) is due to the reduction of electron density around the nuclei due to solvent polarization.

Anisotropy: Large changes in the chemical anisotropy parameter (δ) during the conversion of DHA to VHF were introduced as an accurate indicator to identify structural changes during the switching process.

5. According to the results, the $-NH_2$ derivative is the best choice for applications requiring high sensitivity and visible light absorption, and the –CN derivative is the best choice for energy storage applications (MOST) due to the high stability of the VHF form.

The computational results provide valuable insight into how the electronic nature of substituents influences the behavior of the DHA–VHF photoswitch. In general, the presence of electron donating and electron withdrawing groups significantly modifies the energetic balance between the DHA and VHF isomers. These effects can be primarily attributed to changes in electron distribution within the conjugated π system of the molecule. Electron donating substituents increase electron density and enhance delocalization along the conjugated framework, which tends to stabilize the open chain VHF form. In contrast, electron withdrawing groups decrease electron density and generally favor stabilization of the closed ring DHA structure.

The calculated energetic differences between the two isomers further demonstrate that substituent effects play a decisive role in determining the thermodynamic preference of the system. Variations in substituent electronic properties alter the relative stability of the isomers by modifying the extent of π conjugation and charge distribution throughout the molecular framework. As a result, the balance between the DHA and VHF forms can be systematically tuned through appropriate substitution patterns.

In addition to thermodynamic stability, the substituents also influence the kinetic aspects of the switching process. The calculated activation barriers associated with the thermal VHF $\rightarrow$ DHA ring closure reaction show noticeable dependence on the electronic characteristics of the substituents. These variations can be rationalized by considering the electronic reorganization that occurs during the transition state formation. Substituents capable of stabilizing the developing electronic distribution in the transition state can lower the activation energy, whereas groups that destabilize this electronic arrangement may increase the barrier.

Frontier molecular orbital analysis also provides further insight into the observed trends. Changes in the energies and spatial distributions of the HOMO and LUMO orbitals indicate that substitution affects the electronic structure of both DHA and VHF isomers. In particular, modifications in the HOMO–LUMO energy gap suggest that the optical absorption properties of these systems can be tuned through substituent engineering. Such tunability is highly desirable for optimizing the photochemical performance of DHA–VHF photoswitches.

Overall, the present computational investigation highlights the crucial role of substituent electronic effects in controlling both the thermodynamic and kinetic aspects of the DHA–VHF interconversion. The results demonstrate that rational molecular design through appropriate choice of electron donating and electron withdrawing groups can effectively modulate the energetic landscape and electronic properties of this photochromic system. These findings provide useful guidelines for the development of improved DHA based photoswitches with tailored stability and enhanced functionality for applications in photoresponsive materials and

[Downloaded from mail.ijop.ir on 2026-11-26]

molecular solar thermal energy storage systems.

V. Conclusion

In this work, the effect of electron donating and electron withdrawing substituents on the structural, energetic, and electronic properties of the dihydroazulene–vinylheptafulvene (DHA–VHF) photoswitch was investigated using quantum chemical calculations. The results indicate that the nature of the substituent plays a crucial role in modulating the relative stability of the DHA and VHF isomers as well as the energy barrier associated with the thermal back conversion process.

Electron donating substituents generally enhance the stabilization of the conjugated VHF structure by increasing electron density along the π system, which can lead to a reduction in the energy gap between the two isomers and influence the kinetics of the thermal ring closure reaction. In contrast, electron withdrawing groups tend to stabilize the DHA form and can increase the activation barrier for the VHF→DHA conversion depending on their position and strength.

The calculations further reveal that substituent effects significantly influence the frontier molecular orbitals and the optical properties of the DHA–VHF system. Changes in the HOMO–LUMO gap and electronic distribution suggest that appropriate substitution can shift absorption characteristics and tune the photochemical behavior of the photoswitch.

Overall, the results demonstrate that rational substitution provides an effective strategy for controlling the energetic landscape and photophysical properties of the DHA–VHF system. These findings contribute to the molecular design of improved DHA based photoswitches with tailored stability and energy storage characteristics for potential applications in photoresponsive materials and molecular solar thermal energy storage.

References

[1] R.H. Mitchell, "The metacyclophanediene-dihydropyrene photochromic switch," Eur. J. Org. Chem., pp. 2695–2703, 1999.

[2] H. Bouas-Laurent and H. Dürr, "Organic photochromism," Pure Appl. Chem., Vol. 73, No. 4, pp. 639–665, 2001.

[3] A. Bakkar, F. Lafolet, M. Boggio-Pasqua, D. Jouvenot, E. Saint-Aman, and S. Cobo, "Electrochemical control of the switching process of photochromic dimethyldihydropyrene derivatives," Chem. Commun., Vol. 53, pp. 9360–9363, 2017.

[4] S. Cobo, F. Lafolet, E. Saint-Aman, C. Philouze, C. Bucher, S. Silvi, A. Credi, and G. Royal, "Reactivity of a pyridinium-substituted dimethyldihydropyrene switch under aerobic conditions: Self-sensitized photo-oxygenation and thermal release of singlet oxygen," Chem. Commun., Vol. 51, pp. 13886–13889, 2015.

[5] M. Boggio-Pasqua, M. López Vidal, and M. Garavelli, "Theoretical mechanistic study of self-sensitized photo-oxygenation and singlet oxygen thermal release in a dimethyldihydropyrene derivative," J. Photochem. Photobiol. A, Vol. 333, pp. 156-164, 2017.

[6] R.H. Mitchell, T.R. Ward, Y. Wang, and P.W. Dibble, "Pi-switches: Synthesis of three-way molecular switches based on the dimethyldihydropyrene–metacyclophanediene valence isomerization," J. Am. Chem. Soc., Vol. 121, pp. 2601–2602, 1999.

[7] N. Vilà, G. Royal, F. Loiseau, and A. Deronzier, "Photochromic and redox properties of bisterpyridine ruthenium complexes based on dimethyldihydropyrene units as bridging ligands," Inorg. Chem., Vol. 50, pp. 10581-10591, 2011.

[8] Y. Shao, Z. Gan, E. Epifanovsky, A.T.B. Gilbert, M. Wormit, J. Kussmann, A.W. Lange, A. Behn, J. Deng, X. Feng, D. Ghosh, M. Goldey, P.R. Horn, L. Jacobson, I. Kaliman, R. Khaliullin, T. Kuś, A. Landau, J. Liu, E. Proynov Y. Rhee, R.M. Richard, M.A. Rohrdanz, R.P. Steele, E.J. Sundstrom, H.L. Woodcock, P.M. Zimmerman, D. Zuev, B. Albrecht, E. Alguire, B. Austin, G.J.O. Beran, Y.A. Bernard, E. Berquist, K. Brandhorst, K. Bravaya, S. Brown, D. Casanova, C.-M. Chang, Y. Chen, S.H, Chien, K.D. Closser, D.

[Downloaded from mail.ijop.ir on 2026-11-26]

Crittenden, M. Diedenhofen, R. Distasio, H. Do, A.D. Dutoi, R.G. Edgar, S. Fatehi, L. Fusti, A. Ghysels, A. Golubeva-Zadorozhnaya, J. Gomes, M. Hanson-Heine, P.H.P. Harbach, A.W. Hauser, E.G. Hohenstein, Z.C. Holden, T.-C. Jagau, H. Ji, B. Kaduk, K. Khistyaev, J. Kim, J. Kim, R.A. King, P. Klunzinger, D. Kosenkov, T. Kowalczyk, C. Krauter, K.U. Lao, A.D. Laurent, K.V. Lawler, S.V. Levchenko, C.Y. Lin, F. Liu, E. Livshits, R.C. Lochan, A. Luenser, P.U. Manohar, S.F. Manzer, S.-P. Mao, N. Mardirossian, A.V. Marenich, S.A. Maurer, N. Mayhall, E. Neuscamman, C.M. Oana, R. Olivares-Amaya, D.P. O'Neill, J.A. Parkhill, T.M. Perrine, R. Peverati, A. Prociuk, D.R. Rehn, E. Rosta, N.J. Russ, S.M. Sharada, S. Sharma, D.W. Small, A. Sodt, T. Stein, D. Stück, Y.-C. Su, A.J.W. Thom, T. Tsuchimochi, V. Vanovschi, L. Vogt, O. Vydrov, T. Wang, M.A. Watson, J. Wenzel, A. White, C.F. Williams, J. Yang, S. Yeganeh, S.R. Yost, Z.-Q. You, I.Y. Zhang, X. Zhang, Y. Zhao, B.R. Brooks, G.K.L. Chan, D.M. Chipman, C.J. Cramer, W.A. Goddard, M.S. Gordon, W.J. Hehre, A. Klamt, H.F. Schaefer, M.W. Schmidt, C.D. Sherrill, D. Truhlar, A. Warshel, X. Xu, A. Aspuru-Guzik, R. Baer, A. Bell, N. Besley, J.-D. Chai, A. Dreuw, B. Dunietz, T.R. Furlani, S.R. Gwaltney, C.-P. Hsu, Y. Jung, J. Kong, D.S. Lambrecht, W. Liang, C. Ochsenfeld, V.A. Rassolov, L. Slipchenko, J.E. Subotnik, T.V. Voorhis, J.M. Herbert, A.I. Krylov, P. Gill, and M. Head-Gordon, "Advances in molecular quantum chemistry contained in the Q-Chem 4 program package," Mol. Phys., Vol. 113, pp. 184–215, 2015.

[9] M.J. Frisch, G.W. Trucks, H.B. Schlegel, G.E. Scuseria, M.A. Robb, J.R. Cheeseman, G. Scalmani, V. Barone, G.A. Petersson, H. Nakatsuji, Marco Caricato, H.P. Hratchian, and A.F. Izmaylov, Gaussian 09 Revision C 01 Inc., Wallingford, CT, USA, 2009.

[10] J. Tomasi, B. Mennucci, and R. Cammi, "Quantum mechanical continuum solvation models," Chem. Rev., Vol. 105, No. 8, pp. 2999–3093, 2005.

[11] Y. Kurashige, T. Nakajima, S. Kurashige, K. Hirao, and Y. Nishikitani, "Theoretical investigation of the excited states of coumarin dyes for dye-sensitized solar cells," J. Phys. Chem. A, Vol. 111, No. 25, pp. 5544–5548, 2007.

[12] H.P. Gümüş, Ö. Tamer, D. Avcı, and Y. Atalay, "Effects of donor–acceptor groups on the structural and electronic properties of 4-(methoxymethyl)-6-methyl-5-nitro-2-oxo-1,2-dihydropyridine-3-carbonitrile," Spectrochim. Acta A Mol. Biomol. Spectrosc., Vol. 132, pp. 183–190, 2014.

[13] J. Fabian, "TDDFT-calculations of Vis/NIR absorbing compounds," Dyes Pigm., Vol. 84, pp. 36–53, 2010.

[14] A. Ohshima, A. Momotake, and T. Arai, "Photochromism, thermochromism, and solvatochromism of naphthalene-based analogues of salicylideneaniline in solution," J. Photochem. Photobiol. A, Vol. 162, pp. 473-479, 2004.

[15] J. Jayabharathi, V. Thanikachalam, K. Jayamoorthy, and M.V. Perumal, "A physiochemical study of excited state intramolecular proton transfer process luminescent chemosensor by spectroscopic investigation supported by ab initio calculations," Spectrochim. Acta A Mol. Biomol. Spectrosc., Vol. 79, pp. 6–16, 2011.

[16] M.A. Rauf, S. Hisaindee, and N. Saleh, "Spectroscopic studies of keto–enol tautomeric equilibrium of azo dyes," RSC Adv., Vol. 5, pp. 18097–18103, 2015.

[17] M.S. Zakerhamidi, K. Nejati, Sh. Golghasemi Sorkhabi, and M. Saati, "Substituent and solvent effects on the spectroscopic properties and dipole moments of hydroxyl benzaldehyde azo dye and related Schiff bases," J. Mol. Liq., Vol. 180, pp. 225–234, 2013.

[18] H. Joshi, F.S. Kamounah, C. Gooijer, G. van der Zwan, and L. Antonov, "Excited state intramolecular proton transfer in some tautomeric azo dyes and Schiff bases containing an intramolecular hydrogen bond," J. Photochem. Photobiol. A, Vol. 152, pp. 183-191, 2002.

[19] J. Jayabharathi, V. Thanikachalam, M.V. Perumal, and N. Srinivasan, "A physiochemical study of azo dyes: DFT based ESIPT process," Spectrochim. Acta A Mol. Biomol. Spectrosc., Vol. 83, pp. 200–226, 2011.

[20] K. Filipczak, J. Karolczak, P. Lipkowski, A. Filarowski, and M. Ziółek, "Photochromic cycle of 2′-hydroxyacetophenone azine studied by absorption and emission spectroscopy in

[Downloaded from mail.ijop.ir on 2026-11-26]

different solvents," J. Chem. Phys., Vol. 139, pp. 104305(1-11), 2013.



Azar Bagheri received her B.A. and M.A. degrees from Al-Zahra University with first place and her Ph.D. degree in 2005 from Azad university, Science and Research Branch, Tehran, Iran. She is an associate professor of inorganic chemistry at Azad University, Central Tehran Branch, and has been teaching in this department for 29 years. She has published more than 100 scientific research papers. Her interests include the synthesis and investigation of optical properties of nanoparticles, light-matter interactions, and the study of the mechanism of action of anticancer drugs. In these fields, she has supervised about 110 master's and doctoral students.



Malika Pejman, born in 2005, is a third-year medical student at Iran University of Medical Sciences. She is interested in the field of optical biomedicine and is also active in pharmaceutical research in this field.

[Downloaded from mail.ijop.ir on 2026-11-26]